Mat. Res. Soc. Symp. Proc. Vol. 743 © 2003 Materials Research Society

X-Ray Diffraction Analysis of GaN and AlGaN

H. Kang, N. Spencer, D. Nicol, Z.C. Feng, and I. Ferguson*
School of Electrical and Computer Engineering,
Georgia Institute of Technology, Atlanta, GA 30332, U.S.A
*ianf@ece.gatech.edu
S. P. Guo, M. Pophristic, and B. Peres
EMCORE Corporation, 145 Belmont Drive, Somerest, NJ 08873, U.S.A

ABSTRACT

In this paper, threading dislocation densities in GaN and AlGaN epitaxial layers have been evaluated using two different X-ray analysis techniques; a Williamson Hall (WH) plot and reciprocal space mapping (RSM). GaN and AlGaN have crystalline growth composed of columnar structures that can be estimated by coherence length and angular misorientation measured by X-ray. A WH plot can provide information about coherence length and tilt angle from a linear fit to the linewidth of the triple axis rocking curve (000*l*) symmetric reflections. RSM is typically used to obtain this data, but it is more involved in technique. The two dominant components of threading dislocation densities (screw and edge types) in the GaN and AlGaN epitaxial layers were found to be similar by both techniques. The treading dislocation density correlates to the size of columnar structure as determined by coherence length, tilt angle, and twist angle. The effect of Al composition in AlGaN alloys on these dislocation densities was investigated and found to depend on strongly on the type of nucleation layer, GaN or AlN.

INTRODUCTION

GaN-based materials have attracted much attention for optoelectronic device applications where there is a need to operate in the blue-green regime.[1] However, the high threading dislocation density in the III-Nitrides is an issue that encumbers their further development as optoelectronic devices in the ultraviolet.[2] The threading dislocation (TD) density is normally determined using plan view transmission electron microscopy (TEM), however this technique is destructive and typically requires a few days before the this data can be obtained.[3] X-Ray Diffraction (XRD) has been used to obtain functionally equivalent data from some average measurements of crystal microstructure. Since XRD is non-destructive and rapid characterization technique it is the most common technique used to optimize crystalline quality growth parameters. GaN is different to other compound semiconductor materials because it is formed with large areas of crystalline material that are misaligned to each other, a columnar structure (i.e. mosaic structure).[4] Thus an estimate of size of those domains, the average misorientation between them and dislocation density is important in optimizing material growth. High-resolution XRD reciprocal space mapping (RSM) is normally utilized for detailed characterization of such crystalline structures. However, a much quicker and simpler method to obtain similar information utilizes the Williamson-Hall (WH) plot.

In this study of GaN and AlGaN, RSM and WH plot techniques were used to characterize the columnar structures and to evaluate the threading dislocation densities of thin layers grown by MOCVD. These two methods are compared for consistency and to investigate the effect Al composition in AlGaN alloys on dislocation density.

THEORY

Reciprocal space mapping (RSM) of a reflection plane can be plotted by recording equivalent intensities from a series of Ω scans each having different detector position with respect to 2Θ direction (Ω-2Θ scans). Since the linewidth of these scans for RSM are broadened by size (coherence lengths) and angular misorientation (tilt and twist angles) of the columnar structure, the RSM is used to obtain information of the columnar structure. As illustrated in Fig. 1, the lateral coherence length (L_{ll}) is the reciprocal of the component of the FWHM parallel to surface (L_{coh}) in the RSM of an asymmetric reflection.[5] On the other hand, from the RSM of a symmetric (000*l*) reflection plane, the tilt angle (α_{tilt}) is the vertical component of the FWHM ellipse. Lastly, from the RSM of reflection planes in the a-axis direction, the vertical component of the FWHM ellipse is twist angle (α_{twist}).[6,7,8]

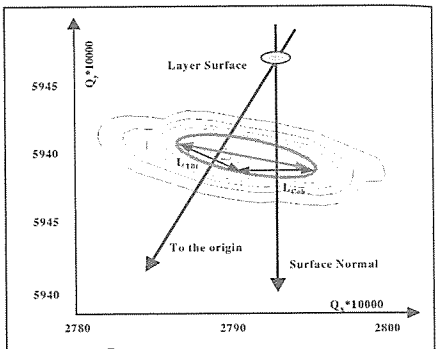

Fig. 1 $(1\bar{1}04)$ RSM of GaN #1. L_{coh} is the length of the FWHM component parallel to surface, and L_{ll} is the reciprocal L_{coh}. α_{tilt} is derived by the length of component perpendicular to origin direction. In addition, α_{tilt} can be obtained from (0004) RSM.

Another technique for obtaining L_{ll} and α_{tilt} is through the use of Williamson-Hall (WH) plots. For this technique, the broadening of the Ω scan (rocking curve) of the symmetric reflections is affected only by the tilt and the coherence length parallel to the reflection surface. WH plots make it possible to distinguish these two broadening mechanisms.[9] When $\beta_\omega(\sin\theta)/\lambda$ is plotted against $(\sin\theta)/\lambda$ for each reflection and a straight line is fitted, the y-intersect (Y_o) of the fitted line is used to estimate the lateral coherence length, L_{ll} (= 0.9 / 2Y_o) [2,10,11,12], where β_ω, θ, and λ are the integral width of the measured profile, the Bragg reflection angle, and X-Ray wavelength, respectively. In addition, the slope of the fitted line corresponds to the tilt angle, α_{tilt}. Additionally, α_{twist} is found from Φ-scan on asymmetric reflections. In this work, it is assumed that columnar structure does not abruptly change over the reflection planes, so the information from a specific reflection by using RSM method can be compared to the mean values obtained from the WH method.

Using the data obtained from RSM or WH method, different dislocation densities can be determined. This is done through the use of Burgers vectors and the calculations given below. GaN layers have three main types of threading dislocation (TD) densities; screw dislocation along the c-axis [0001], edge dislocation in the a-axis $[11\bar{2}0]$ and mixed screw and edge dislocations. In this work the mixed dislocations are ignored because they should have much lower densities than pure screw or edge dislocation. Screw and edge dislocation densities are distinguished by Burgers vectors b_c = [0001] and b_a = ⅓ $[11\bar{2}0]$ respectively. The tilt angle is used to determine the screw dislocation density, N_{screw}, with the Burgers vector $|b_c|$ by [2,11]

$$N_{screw} = \alpha_{tilt}^2 / (4.35 |b_c|^2) \quad (2)$$

The same is done with twist angle to determine the edge dislocation density, N_{edge}, with the Burgers vector $|b_a|$, the majority of the dislocations occur at the small angle grain boundaries, [2]

$$N_{edge} = \alpha_{twist} / (2.1\,|b_a|\,L_{||}) \quad (3)$$

These dislocation density is a function of Burgers vector that is directly expressed by lattice constant of the films. For dislocation densities of $Al_xGa_{1-x}N$ layers, therefore it is necessary to find their lattice constants. Lattice constant of an alloy can be derived using Vegard's law ($a_{AlN\text{-}xGaxN} = xa_{AlN} + (1\text{-}x)a_{GaN}$) which is a relation between composition and lattice constant.[13]

EXPERIMENT

In this work, all samples were grown by Metalorganic Chemical Vapor Deposition (MOCVD) in an EMCORE D180 short jar system on (0001) on sapphire. TMGa, TMAl and NH_3 were used as the source precursors for Ga, Al, and N, respectively. A 30nm low-temp (540 °C at 300 Torr) GaN nucleation layer was used for undoped GaN samples #1, #2, and #3; 2.2, 1.9 and 2.2 um thick, respectively. The GaN epilayers were grown at 1050 °C with a V/III ratio of 4000 and a growth rate of ~2μm/h. a 25 nm low-temperature (590 °C at 300 Torr) AlN nucleation layer was used for AlGaN epilayers. $Al_{0.15}Ga_{0.85}N$ #4 was grown at 900 °C on 2 m GaN buffer layer with a V/III ratio of 33000 and a growth rate of ~0.15 m/h. $Al_{0.4}Ga_{0.6}N$ #5, $Al_{0.62}Ga_{0.38}N$ #6 and AlN sample were grown at 1080 °C on low-temperature AlN nucleation layers with a V/III ratio of 4000 and a growth rate of 0.5, 0.3 and 0.2 μm/h, respectively. In-situ reflectometry was used to monitor the growth rate and the surface morphology.

XRD measurements were performed with the Philips X'pert MRD triple-axis diffractometer equipped with a four bounce Ge (022) monochromator and a Cu sealed anode. Ω scan and 2Θ- Ω scan on the symmetric (0002), (0004), and (0006) reflection planes as well as RSMs on (0004), ($1\bar{1}04$), and ($1\bar{2}11$) reflection planes were performed. In addition, Φ-scans were completed on each sample.

RESULTS

Undoped GaN

A reciprocal space mapping (RSM) of GaN #1 is shown in Figure 1, from which lateral coherence length is determined as the reciprocal of L_{coh}. In addition, the α_{tilt} and α_{twist} are given by (0004) and ($1\bar{2}11$) RSMs (not shown here), respectively. Furthermore, $L_{||}$, α_{tilt}, and α_{twist} are determined in the same manner for GaN #2 and #3.

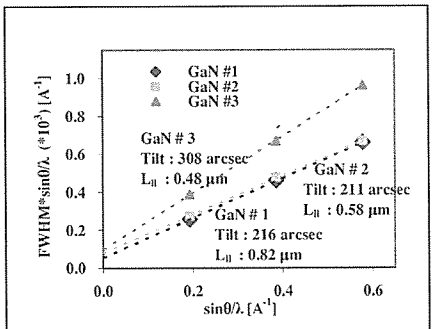

Fig. 2 Williamson-Hall Plots for undoped

WH plots have also been used to extract values for $L_{||}$ and α_{tilt} for these samples in Fig. 2. Values for α_{twist} were obtained directly from Φ-scans on asymmetric reflections.

The data for GaN obtained by both these techniques is summarized in Table 1. The mean N_{screw} with the Burgers vector ($|b_c|$=5.185 Å) and N_{edge} with the Burgers vector ($|b_a|$=3.189 Å) obtained using a WH plot have been compared with these obtained using RSM. The α_{tilt} values by WH are larger than these by RSM methods. This may be explained by annihilation of the defects with respect to the growth direction (i.e. c-axis)

during the growth process.[14, 15] Since the tilt angle along the c-axis is relaxed during growth, the average α_{tilt} by WH is smaller than a transition α_{tilt} value by RSM. While the mean L_{ll} by WH is smaller than a transition L_{ll} value by RSM, since L_{ll}, a component length with respect to

	Method	GaN #1	GaN #2	GaN #3
L_{ll} [um]	WH plot	0.82	0.58	0.48
	RSM	0.33	0.25	0.28
Tilt [aresec]	WH plot	216	211	308
	RSM	274	266	335
Twist [arcsec]	Φ scan	835	662	792
	RSM	792	655	702
N_{scew} [cm^{-2}]	WH plot	9.4E+07	9.0E+07	1.9E+08
	RSM	1.5E+08	1.4E+08	2.3E+08
N_{edge} [cm^{-2}]	WH plot	7.4E+08	8.3E+08	1.2E+09
	RSM	1.7E+09	1.9E+09	1.8E+09

Table 1. Summary of the mosaic structure factors of GaN samples #1, #2, and #3by various methods

parallel to surface, is smaller as α_{tilt} is larger. These differences lead to dissimilarity between two methods for N_{screw} and N_{edge} due to relaxation of defect during growth. The WH plot provides the mean size and angular distribution of the columnar structure from a combination of the (0002), (0004), and (0006) reflections, while RSM provides a specific value from a specific reflection. Therefore, the WH plot may be expected to provide a more reliable estimate of the average values for the columnar structure of GaN, even though RSM measurements will provide more accurate information. It should be noted that the values obtained for N_{screw} and N_{edge} are less accurate than those typically measured by TEM and this is being investigated.[3] However, both the WH plot and RSM still allow a relative measure of material quality.

$Al_xGa_{1-x}N$/Nucleation layer on Al_2O_3

Based on the previous two methods for GaN samples, AlGaN epitaxial layers have also been investigated. Fig.3 exhibits AlGaN #4 RSMs of asymmetric and symmetric reflection planes which provide L_{ll} and α_{tilt}. While α_{twist} is given by $(1\bar{2}11)$ RSMs (not shown here). AlGaN #5 and #6 were also performed in the same way. These RSMs have two peaks corresponding to GaN layer and AlGaN layer, respectively. It can be observed that the GaN peak is stronger than the diffraction corresponding to the AlGaN layer in Fig, 3 (a). A thicker

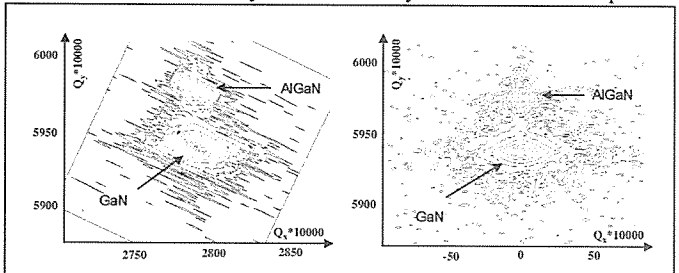

Fig.3 (a) $(1\bar{1}04)$ RSM of AlGaN #4 (b) (0004) RSM of AlGaN #4

layer (2 um GaN > 0.2 um $Al_{0.15}Ga_{0.85}N$) leads to stronger XRD intensity as well as sharper peak.

It is shown in Fig. 4 that WH plots provide $L_{\parallel}$ and α_{tilt}. $Al_{0.15}Ga_{0.85}N$ layer of AlGaN #4 on

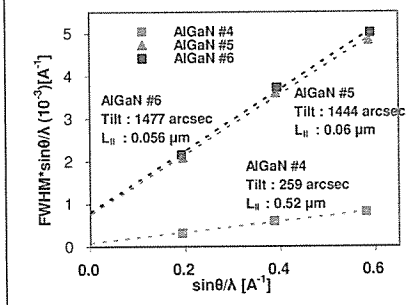

Fig. 4 Williamson-Hall plots for $Al_xGa_{1-x}N$ layers of AlGaN #4, #5, and #6. Different nucleation layer cause this quite difference between AlGAN #4 and AlGaN #5 (or #6)

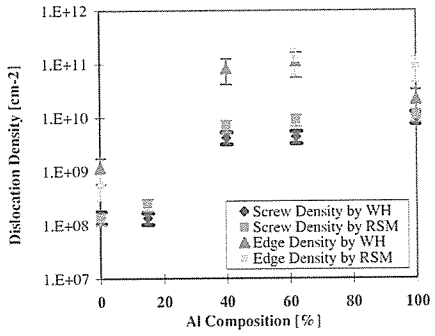

Fig. 5 Screw and edge densities with Al composition for AlGaN #4, #5, and #6

GaN nucleation layer seems to have values similar to those of GaN samples. Whereas, AlGaN #5 and #6 grown AlN nucleation layer have quite different values from the AlGaN #4. The difference is probably caused by relaxation of the underlying layer. This relaxation associated with layer thickness can be influence on the columnar structure of the AlGaN layer and also cracking in this layer.[16] In addition, AlGaN samples have larger tilt angles and smaller coherence lengths as the Al composition increases.

Dislocation density is a function of Burgers vector that is directly indicated by lattice constant of the layer. 2Θ scans on (0004) reflection are measured to evaluate lattice constants of AlGaN #4, #5, and #6. Thus, from the measurement data, the Burgers vectors of c-axis and a-axis for $Al_xGa_{1-x}N$ alloys can be easily determined as $|b_c|$ =5.153 and $|b_a|$=3.177 Å, $|b_c|$=5.101 and

	Methods	AlGaN #4 GaN layer	AlGaN #5 $Al_{0.15}Ga_{0.85}N$ layer	AlGaN #6 $Al_{0.4}Ga_{0.6}N$ layer	AlGaN #6 $Al_{0.62}Ga_{0.38}N$ layer	AlN AlN layer
$L_{\parallel}$ [um]	WH plot	0.51	0.52	0.06	0.056	0.27
	RSM	0.62	0.46	0.05	0.054	0.06
Tilt [arcsec]	WH plot	265	259	1444	1477	2140
	RSM	256	349	1857	2120	2232
Twist[arcsec]	Φ scan	831	NA	6804	8496	8028
	RSM	493	NA	NA	9457	7380
N_{screw} [cm^{-2}]	WH plot	1.4E+08	1.4E+08	4.3E+09	4.4E+09	1.0E+10
	RSM	1.3E+08	2.5E+08	7.2E+09	9.5E+09	1.1E+10
N_{edge}[cm^{-2}]	WH plot	1.2E+09	NA	8.3E+10	1.1E+11	2.2E+10
	RSM	5.8E+08	NA	NA	1.3E+11	9.0E+10

Table 2. Summary of the mosaic structure factors of AlGaN samples #4, #5, and #6 by various methods

$|b_a|$=3.158 Å, and $|b_c|$=5.055 and $|b_a|$=3.141 Å for AlGaN samples #4, #5, and #6, respectively.

The variation of the screw and edge densities with Al composition measured by WH and RSM is shown in Figure 5. It is apparent that AlGaN grown on the GaN nucleation layer (< 40% Al) shows lower densities of screw and edge dislocations than those grown on AlN nucleation layers (> 40% Al). Moreover, it appears that the screw density increase with Al composition in $Al_xGa_{1-x}N$ layer (> 40% Al) shows a systematic increase with Al composition. It could be expected that the growth mechanism could change with increasing Al however further measurements are needed before this conclusion can be reached.

Table 2 shows mean geometric size of columnar structures as well as dislocation densities for the epitaxial AlGaN layers. Some values are not reported due to the weak XRD intensity and, as a consequence, the large error on these measurements. Moreover, the values obtained for L_{II}, α_{tilt} and α_{twist} by WH and RSM are in closer agreement than GaN; i.e. specific values aren't much varied since defects are less relaxed due to smaller thickness and different type of nucleation layers.

CONCLUSION

In this work, we have studied the typical mosaic structures of GaN on sapphire with WH and RSM methods by XRD measurements. The effects of not only the columnar structure's size and angular uniformity, but Al composition in the epitaxial AlGaN layers on TD density have been investigated. In Addition, TD is influence by the type and thickness of nucleation layer

Acknowledgements

This work was funded by DARPA (John Carrano) and ONR (Yoon-Soo Park) under contract number N00014-02-1-0596 as part of the SUVOS program.

REFERENCES

[1] C. Kim, and J. Je, Mat.Res. Soc. Symp.**595**, W3.52.1 (2000)
[2] T. Metzger, R. Hopler, E. Born, and O. Ambacher, Phil. Mag. A, **77**, 1013 (1998)
[3] F. Ponce, *Microstructure of Epitaxial III-V Nitride Thin Films*, 1997, p.141
[4] T. Cheng, L. Jenkins, S. Hooper, and C. Foxon, Appl. Phy. Lett. **66**, 1509 (1995)
[5] P.F. Fewster, X-Ray Scattering from semiconductors 263 (2000)
[6] P.F. Fewster, *X-Ray and Neutron Dynamical Diffraction: Theory and Applications, NATO ASI Series B*: Physics **357** (1996) p.287
[7] P.R. Fewster, N. L. Andrew, and C.T. Foxon, J. Crys. Growth **230**, 404, (2001)
[8] D.K. Bowen, *High Resolution X-ray Diffractometry and Topography*, 149 (2001)
[9] G.K. Williamson and W.H. Hall, Acta. Metall. **1**, 22 (1953)
[10] T. Metzger, R. Hopler, E. Born, and S. Christiansen, Phys. Stat. Sol. A **162**, 529 (1997)
[11] H.Wang, J. Zhang, C. Chen, Q. Fareed, and J. Yang, Appl. Phys. Lett., **81**, 605 (2002)
[12] H. Heinke, V. Kirchner, S. Einfeldt, and D. Hommel, Phys. Stat. Sol. A **172**, 391 (1999)
[13] P.Bhattacharya, *Semiconductor Optoelectronic Devices*, (1997), p.5
[14] S. Molina, A. Sanchez, F. Pacheco, and R. Garcia, Appl. Phys. Lett. **74**, 3362 (1999)
[15] L. Kirste, D. Ebling, C. Haug, and K. Tillmann, Mater. Sci. Eng., B **82** 9 (2001)
[16] B. Bennett, Appl. Phys. Lett. **73**, 3736 (1998)